Immunology and Inflammation

Ym1 protein crystals promote type 2 immunity

Ines Heyndrickx, Kim Deswarte, Kenneth Verstraete, Koen H. G. Verschueren, Ursula Smole, Helena Aegerter, Ann Dansercoer, Hamida Hammad, Savvas N. Savvides, Bart N. Lambrecht

Laboratory of Immunoregulation and Mucosal Immunology, VIB-UGent Center for Inflammation Research, Ghent, Belgium • Department of Internal Medicine and Pediatrics, Ghent University, Ghent, Belgium • Unit for Structural Biology, VIB-UGent Center for Inflammation Research, Ghent, Belgium • Department of Biochemistry and Microbiology, Ghent University, Ghent, Belgium • Department of Pulmonary Medicine, Erasmus University Medical Center Rotterdam, Rotterdam, The Netherlands

Reviewed Preprint

Revised by authors after peer review.

About eLife's process

Reviewed preprint version 2
December 21, 2023 (this version)

Reviewed preprint version 1
October 4, 2023

Sent for peer review
July 28, 2023

Posted to preprint server
July 3, 2023

Abstract

Spontaneous protein crystallization is a rare event, yet protein crystals are frequently found in eosinophil-rich inflammation. In humans, Charcot-Leyden crystals (CLCs) are made from galectin-10 (Gal10) protein, an abundant protein in eosinophils. Whereas mice do not encode Gal10 in their genome, they do form pseudo-CLCs, made from the chitinase-like proteins Ym1 and/or Ym2, encoded by *Chil3* and *Chil4* and made by myeloid and epithelial cells respectively. Here, we investigated the biological effects of pseudo-CLCs since their function is currently unknown. We produced recombinant Ym1 crystals which were shown to have identical crystal packing and structure by X-ray crystallography as *in vivo* native crystals derived from murine lung. When administered to the airways of mice, crystalline but not soluble Ym1 stimulated innate and adaptive immunity and acted as a type 2 immune adjuvant for eosinophilic inflammation via triggering of dendritic cells (DCs). Murine Ym1 protein crystals found at sites of eosinophilic inflammation reinforce type 2 immunity and could serve as a surrogate model for studying the biology of human CLCs.

eLife assessment

This is an **important** and interesting account of the ability of Ym1 crystals to promote type 2 immunity in vivo, in mice. The data presented are **compelling**, building on and significantly advancing evidence this group has previously published on the type 2 immunogenicity of other protein crystals. The work will be of relevant interest to immunologists and researchers working on type 2 inflammatory disease, in the lung and in others tissues.

Introduction

Protein crystals have been described already 150 years ago in eosinophilic inflammatory lesions in humans by Charcot and von Leyden [1-3]. Most proteins can only function properly in the soluble state and spontaneous protein crystallization *in vivo* remains a rare and largely unsolved

scientific enigma [4,5].

Protein crystals have also been documented in mouse tissues, almost exclusively in the context of type 2 inflammation, rich in eosinophils, T helper 2 (Th2) cells and alternatively activated macrophages [6-22]. Such crystals in mice are colorless, but in histochemical stains they stain brightly with eosin, consistent with their protein content [14]. Before their biochemical nature was elucidated, they were therefore often referred to as eosinophilic crystals [6]. These murine crystals are frequently observed in aged mice and genetically altered mice on a C57BL/6 or Sv/129 background, and in the context of eosinophil-rich asthma and parasitic infections [6,23]. Although eosinophilic crystals have been documented in the skin, biliary tree, stomach, lymph nodes, spleen and bone marrow of mice, it is clear that the principal site of crystal accumulation is in the lung. In several descriptions, accumulation of eosinophilic crystals was associated with severe lung inflammation and the disease was called eosinophilic crystalline pneumonia, acidophilic macrophage pneumonia or crystalline pneumonitis [7,17,23,24]. In histology slides, the accumulated crystals are variable in size and shape ranging from needle-like crystals to rectangular plates [14]. Their resemblance to the needle-shaped human Charcot-Leyden crystals (CLCs) frequently resulted in the incorrect identification of these murine crystals as CLCs [24,25]. However, only in 2000, almost 100 years after they were first described, Guo *et al.* purified crystals from the bronchoalveolar lavage (BAL) fluid of viable motheaten (me^v/me^v) mice and mass spectrometry analysis identified the chitinase-like protein (CLP) Ym1 as the sole protein component [6], thereby providing an unambiguous annotation of their content and distinguishing them from CLCs. Human CLCs are comprised of the eosinophil-derived galectin-10 (Gal10) protein, which is not encoded in the mouse genome [26,27]. Ym1 is mainly produced by alveolar macrophages, alternatively activated “M2” macrophages, neutrophils and a subset of circulating pro-repair monocytes [28-30]. In hyaline gastric lesions of aged 129S4/SvJae and B6,129 CYP1A2 null mice, pseudo-CLCs were found to consist of the closely related CLP Ym2, which is a protein mainly made by epithelial cells under the influence of IL-13 [14,25,31,32]. Ym1 (encoded by the *Chil3* gene) and Ym2 (encoded by the *Chil4* gene) are CLPs belonging to the glycoside hydrolase family 18 (GH18) and are unique to mice, with no known human orthologues [33]. Their potential receptors and natural binding partners are largely unknown, as are the exact functions of these still very enigmatic proteins. We previously reported that recombinant Gal10 crystals produced *in vitro* showed crystal packing and structure identical to CLCs derived from patient mucus. When administered to the airways of mice, Gal10 crystals stimulated innate and adaptive immunity and acted as a type 2 adjuvant [34]. Since mice do not encode the *LGALS10* gene, Gal10 has the potential to act as a neo-antigen in this setting. Here, we tested the *in vivo* relevance of pseudo-CLCs since these are made endogenously in mice at sites of eosinophilic inflammation, albeit mainly by macrophages and epithelial cells. We showed that recombinant *in vitro* made Ym1 and Ym2 crystals were structurally similar to crystals isolated from mice and to each other, and when administered to the airways of mice, crystalline Ym1, but not soluble Ym1 protein stimulated innate and adaptive immunity and acted as an adjuvant for Th2 driven eosinophilic airway inflammation and immunoglobulin secretion.

Materials and methods

Mice

Female wild type (WT) C57BL/6 mice were purchased from Janvier Labs (Saint-Berthevin, France), housed under specific pathogen-free conditions and used between 6 and 8 weeks of age. Investigators were not blinded to group allocation during experiments. No animals were excluded from the analysis. All experiments were approved by the animal ethics committee at Ghent University and were in accordance with Belgian animal protection law.

Production of recombinant Ym1 and Ym2 protein and crystals

A synthetic codon-optimized DNA sequence (Genscript) encoding murine Ym1 (Uniprot ID O35744, residues 22 – 398) was cloned in the pCAGG mammalian expression vector in frame with the mouse IgH signal peptide (MGWSCIIFFLVATATGVHS). A synthetic codon-optimized DNA sequence (Genscript) encoding murine Ym2 (Uniprot Q91Z98, residues 22 - 402) was cloned in the pTwist-CMV-BetaGlobin mammalian expression vector (Twist Biosciences) in frame with the mouse IgH signal peptide (MGWSCIIFFLVATATGVHS), and an N-terminal hexahistine-tag followed by a Tobacco Etch Virus (TEV)-protease cleavage site.

Ym1 and Ym2 were produced in FreeStyle 293-F cells in suspension. Cells were transfected with 1 µg/ml DNA using 2-fold excess of linear polyethylenimine (PEI; Polysciences). Conditioned medium containing the secreted recombinant protein was collected 4 days post transfection and filtered. Medium containing Ym1 was dialyzed to 20 mM Tris pH 8.0 and the Ym1 protein was purified via Q Sepharose anion exchange chromatography. Ym1 was further purified to a pure solution via size-exclusion chromatography using phosphate-buffered saline (PBS) as running buffer. Ym2 was purified from the clarified conditioned medium via immobilized metal affinity chromatography (IMAC) and size-exclusion chromatography with PBS buffer. Endotoxin levels were determined with an Endosafe-PTS system (Charles River) to be lower than 1 EU/mg of recombinant protein. To form recombinant Ym1 crystals, recombinant Ym1 protein (3 to 4 mg/ml) was incubated with 1M Na-acetate buffer pH 4.6 with a buffer:target protein ratio of 1:10 (v/v). During a 24h incubation the protein solution was agitated a few times by inverting it five times, after which the solution turned cloudy due to the formation of protein crystals. The crystal-containing suspension was spun down (400g for 5 min) and washed three times with sterile and endotoxin-free PBS before the crystals were resuspended in 1 ml of sterile and endotoxin-free PBS. The total protein concentration of this solution was determined by solubilizing 20 µl of the crystal suspension in an equal volume of 6M guanidinium hydrochloride and measuring the absorbance at 280 nm with a Thermo Scientific NanoDrop 2000. The calculated extinction coefficient for Ym1 was 77155 M^{-1} cm^{-1}.

Crystallographic structure determination of *ex vivo* and recombinant Ym1 and Ym2 crystals

Single *ex vivo* Ym1 and Ym2 crystals were harvested from the BAL fluid of me^{v}/me^{v} mice and C57BL/6J-Tg(CAG-Gal10)^{Bla} mice by using mounted cryo-loops. Before being cryo-cooled in liquid nitrogen, crystals were cryo-protected by a brief soak in PBS supplemented with 35% (v/v) ethylene glycol (Ym1) or 35 % glycerol (Ym2). Recombinant Ym1 was crystallized in condition A7 of the Hampton Research Crystal Screen HT (0.1 M sodium cacodylate pH 6.5, 1.4 M sodium acetate) via vapor diffusion sitting drop crystallization experiments, and crystals were cryo-protected with mother liquor supplemented with 30% (v/v) glycerol. Following overnight incubation with TEV-protease, recombinant Ym2 was crystallized via vapor diffusion sitting drop crystallization experiments using 0.1 M sodium acetate pH 6.0 and 200 mM $CaCl_2$ as mother liquor, and crystals were cryoprotected with 30% (v/v) PEG-400. Diffraction experiments at 100 K were conducted on beamlines Proxima 1 (SOLEIL synchrotron, Saint-Aubin, France), P14 of Petra III (DESY, Hamburg, Germany) and X06SA (PXI) of the Swiss Light Source (Paul Scherrer Institute, Villigen, Switzerland). All data were integrated and scaled using the XDS suite[35] and the CCP4 suite [36]. Molecular replacement was executed using Phaser [37] employing the structure of Ym1 (pdb: 1vfb) as a search model. Further rebuilding of the model and refinement was performed in *COOT* [38] and autoBuster [39]. Map and model validation was monitored throughout the refinement procedure using *COOT*, the CCP4 package and PDB_REDO server [40].

In vivo models

To analyze the innate immune responses, WT C57BL/6 mice were injected intratracheally (i.t.) with 100 µg Ym1 crystals or 100 µg soluble Ym1 diluted in 80 µl of PBS. After 6 and 24 hours, mice were euthanized by CO_2 inhalation or an overdose of pentobarbital (KELA Laboratoria) and BAL fluid and lungs were collected.

To analyze dendritic cell (DC) activation, WT C57BL/6 mice were injected i.t. with 5 µg Alexa Fluor 488-labeled ovalbumin (OVA-AF488) mixed with 100 µg Ym1 crystals or with 100 µg soluble Ym1 diluted in 80 µl of PBS. After 24 hours, mice were euthanized by CO_2 inhalation and mediastinal lymph nodes (mLNs) were collected.

To analyze the adaptive cellular immune responses, CD4+ OT-II KN2 cells were purified from CD45.1.2 OT-II KN2 donor mice with the MojoSort™ Mouse CD4 T Cell Isolation Kit (Biolegend) and labeled with cell proliferation dye eFluor 450 (0.01 mM; Thermo Fisher Scientific) for 10 min in the dark at 37°C. Next, 1×10^6 of these labeled cells (in 100 µl of PBS) were injected intravenously (i.v.) into WT C57BL/6 mice and subsequently, mice were injected i.t. with 10 µg ovalbumin (OVA, Worthington) or with 10 µg OVA mixed with 100 µg of Ym1 crystals or 100 µg soluble Ym1 (in 80 µl of PBS). For this experiment, OVA was pre-filtered through a 0.22 µm filter. On day 4 and 7, mice were euthanized by CO_2 inhalation and mLNs and lungs were collected.

To analyze the adaptive humoral immune responses, WT C57BL/6 mice were injected intraperitoneally (i.p.) on day 0 with 0.5 mg Ym1 crystals or 0.5 mg soluble Ym1, on day 7 with 0.5 mg Ym1 crystals and on day 14 with 0.5 mg Ym1 crystals or 10 µg Sol Ym1 all diluted in 500 µl PBS. On day 21 mice were euthanized with an overdose of pentobarbital (KELA Laboratoria) and blood was collected.

To analyze the type 2 adjuvanticity of Ym1 crystals, WT C57BL/6 mice were sensitized i.t. on day 0 and day 1 with 100 µg OVA (Worthington), 100 µg OVA mixed with 100 µg of Ym1 crystals or 100 µg OVA mixed with 100 µg soluble Ym1 diluted in 80 µl PBS. On days 11 to 13, all mice were challenged daily intranasally (i.n.) with 20 µg of OVA (Worthington) diluted in 40 µl of PBS. One day after the last challenge, on day 14, mice were euthanized with an overdose of pentobarbital (KELA Laboratoria) and blood, BAL fluid and mLNs were collected.

All i.t. and i.n. treatments were given after mice were anesthetized with isoflurane (2 liters/min, 2 to 3%; Abbott Laboratories).

Blood was obtained from the iliac vein and centrifuged at 10000 rpm for 10 min at room temperature (RT). Serum was collected and stored at −20 °C until further use (serum antibody ELISA). BAL was performed by injecting PBS containing 0.01 mM EDTA (Lonza) through a tracheal canula. Subsequently, BAL fluid was centrifuged (400g for 5 min at 4°C). The supernatant was collected and stored at −20°C until further use (cytokine ELISA) and the pellet was used for ImageStream or flow cytometry. To obtain lung and mLN single-cell suspensions for flow cytometry, lungs and mLNs were first cut with a scissor and then digested at 37°C for 30 or 15 min respectively in RPMI-1640 (ThermoFisher Scientific) containing Liberase TM (20 µg/ml; Merck) and deoxyribonuclease (DNase) I (0.01 U/µl; Merck). The resultant cell suspensions were filtered through a 70 µm filter. To obtain mLN single-cell suspensions for flow cytometry or mLN restimulation cultures, mLNs were smashed on a 70 µm filter. To measure pro-inflammatory cytokines, lungs were snap frozen in liquid nitrogen and homogenized with a TissueLyser II from Qiagen in tissue lysis buffer [40 mM tris-HCL (pH 6.8), 275mM NaCl and 20% glycerol (Sigma-Aldrich)]. One tablet of PhosSTOP (Sigma-Aldrich) and one tablet of Complete ULTRA tablets, Mini, Easypack (Sigma-Aldrich) were added per 10 ml of tissue lysis buffer. After homogenization, 2% IGEPAL CA-630 (U.S. Biological) was added. Subsequently, the samples were rotated for 30 min and

centrifuged (20000g for 10 min at 4°C). Supernatants were stored at −20°C. The total protein concentration was measured with the NanoOrange protein quantitation kit from Thermo Fisher Scientific.

Flow cytometry

Prior to staining for flow cytometry, single-cell suspensions were depleted of red blood cells (RBCs) by using RBC lysis buffer [0.15 M NH4Cl (Merck), 1 mM KHCO3 (Merck), and 0.1 mM Na2-EDTA (Merck) in MilliQ H2O] produced in-house. For all flow experiments, single cell suspensions were incubated with the eBioscience™ Fixable Viability Dye eFluor™ 506 (ThermoFisher Scientific) to identify dead cells. Fc Block 2.4.G2 (Bioceros) was used to block aspecific antibody binding. Cell surface markers were stained for 30 min at 4°C in the dark. 123count eBeads™ Counting Beads (ThermoFisher Scientific) were added to each sample to determine absolute cell numbers. Settings were calibrated using UltraComp eBead™ Compensation Beads (ThermoFisher Scientific). Data were acquired on an LSR Fortessa with FACS Diva software (BD Biosciences) and were analyzed with FlowJo software (Tree Star).

For the analysis of innate immune responses, lung single-cell suspensions were stained for flow cytometry using FITC-conjugated anti-Ly-6C (AL-21) (BD Biosciences), PE-conjugated anti-Siglec-F (E50-2440) (BD Biosciences), PE-Cy5-conjugated anti-CD3e (145-2c11) (Thermo Fisher Scientific), PE-Cy5-conjugated anti-CD19 (1D3) (Thermo Fisher Scientific), PE-Cy7-conjugated anti-CD11c (N418) (Thermo Fisher Scientific), BD Horizon V450-conjugated anti-CD11b (M1/70) (BD Biosciences), Brilliant Violet 605-conjugated anti-CD45 (30-F11) (BD Biosciences), Alexa Fluor 647-conjugated anti-CD64 (X54-5/7.1) (BD Biosciences), Alexa Fluor 700– conjugated anti-Ly6G (1A8) (BD Biosciences) and APC-eFluor 780–conjugated anti-I-A/I-E (M5/114.15.2) (Thermo Fisher Scientific).

For the analysis of DC activation, mLN single-cell suspensions were stained for flow cytometry using PerCP-Cy5.5-conjugated anti-CD80 (16-10A1) (BioLegend), eFluor 450-conjugated anti-CD11c (N418) (ThermoFisher Scientific), Brilliant Violet 650-conjugated anti-XCR1 (ZET) (BioLegend), Brilliant Violet 711-conjugated anti-CD64 (X54-5/7.1) (BioLegend), Alexa Fluor 647-conjugated anti-CD172a (P84) (BioLegend), Alexa Fluor 700-conjugated anti-Ly-6C (AL-21) (BD Biosciences), APC-eFluor 780-conjugated anti-MHCII (M5/114.15.2) (ThermoFisher Scientific), PE-conjugated anti-CD88 (20/70) (BioLegend), biotin-conjugated anti-CCR7 (4B12) (ThermoFisher Scientific) + PE-CF594-conjugated streptavidin (BD Biosciences), PE-Cy5-conjugated anti-CD3e (145-2c11) (ThermoFisher Scientific), PE-Cy5-conjugated anti-CD19 (1D3) (Thermo Fisher Scientific), PE-Cy7-conjugated anti-CD86 (PO3) (BioLegend), BUV395-conjugated anti-CD11b (M1/70) (BD Biosciences) and BUV737-conjugated anti-CD26 (H194-112) (BD Biosciences).

For T cell response analysis, mLN and lung single-cell suspensions were stained using FITC-conjugated anti-Va2 TCR (B20.1) (BD Biosciences), Brilliant Violet 605-conjugated anti-CD45.1 (A20) (BioLegend), RedFluor710-conjugated anti-CD44 (IM7) (Thermo Fisher Scientific), APC-eFluor780-conjugated anti-CD25 (PC61.5) (Thermo Fisher Scientific), PE-conjugated anti-CD62L (MEL-14) (BD Biosciences), biotin-conjugated anti-hCD2 (RPA-2.10) (BioLegend) + PE-CF594-conjugated streptavidin (BD Biosciences), PE-Cy7-conjugated CD3e (145-2C11) (BioLegend), BUV395-conjugated anti-CD4 (GK1.5) (BD Biosciences) and BUV737-conjugated anti-CD45.2 (104) (BD Biosciences).

BAL cells were stained with PE-conjugated anti-Siglec F (E50-2440) (BD Biosciences), PE-Cy5-conjugated anti-CD3e (145-2c11) (ThermoFisher Scientific), PE-Cy5-conjugated anti-CD19 (1D3) (Thermo Fisher Scientific), PE-Cy7-conjugated anti-CD11c (N418) (ThermoFisher Scientific), BD Horizon V450-conjugated anti-CD11b (M1/70) (BD Biosciences), Alexa Fluor 700-conjugated anti-Ly6G (1A8) (BD Biosciences) and APC-eFluor 780-conjugated anti-MHCII (M5/114.15.2) (Thermo Fisher Scientific).

ImageStream

For ImageStream analysis, the pellets obtained after centrifugation of the BAL fluid were pooled and stained for 30 min at 4°C with unconjugated polyclonal goat anti-mouse Ym1/2 (AF2446, R&D Systems; 1:100 diluted in PBS). After washing, the pellet was stained for 30 min at 4°C in the dark with Alexa Fluor 647-conjugated polyclonal donkey anti-goat IgG (ThermoFisher Scientific; 1:1000 diluted in PBS). Fc Block 2.4.G2 (Bioceros) was used to block aspecific antibody binding. Data were acquired on an Amnis ImageStreamX Mk II with INSPIRE™ software (Luminex) and were analyzed with IDEAS® software (Luminex).

Enzyme-linked immunosorbent assay (ELISA)

Interleukin (IL)-1β, IL-5, IL-6, IL-10, IL-13, IL-33, tumor necrosis factor alpha (TNFα) and C-C motif chemokine ligand 2 (CCL2) concentrations were evaluated using the Ready-SET-Go!™ ELISA kits (ThermoFisher Scientific). CCL24 concentrations were evaluated using the Mouse CCL24/Eotaxin-2/MPIF-2 DuoSet ELISA kit (R&D Systems). Serum Ym1-specific immunoglobulin M (IgM) and OVA-specific immunoglobulin G1 (IgG1) antibody levels were determined in flat-bottom 96-well plates (Greiner Bio-One), coated overnight with 0.1 mg/ml soluble Ym1 in PBS or with 0.1 mg/ml OVA (Worthington) in 0.1 M sodium carbonate buffer (pH 9.5), respectively. After washing and blocking for 1 hour, the samples diluted in PBS were added in duplicate and incubated for 2.5 hours at RT. After washing, biotinylated anti-mouse IgG1 or IgM detecting antibody (0.5 mg/ml; BD Biosciences) plus streptavidin-HRP reagent (1:250; BD Biosciences) was added and incubated for 1 hour at RT. After another wash step, 1× TMB substrate solution (Thermo Fisher Scientific) was added and to stop the reaction, 2.5N H_2SO_4 was used. Finally, the absorbance was read at 450 nm (and 650 nm as reference) with a Perkin Elmer multilabel counter and data were collected with Wallac 1420 Manager software (PerkinElmer).

Statistical analysis

Experiments shown in **Figure 2** were analyzed with an ordinary two-way ANOVA test with Tukey's multiple comparisons test. For all experiments in **Figure 3**, **4** and **5**, the normality of each group was first checked by using the Shapiro-Wilk statistical test. Parametric data were analyzed with an ordinary one-way ANOVA test with Šidák's multiple comparison correction and nonparametric data were analyzed with a Kruskal-Wallis test with Dunn's multiple comparison correction. All statistical tests were performed in GraphPad Prism software (GraphPad Software).

Supplementary Online Material

This paper has an online data **supplement. Table S1** describes the key crystallographic data of *ex vivo* isolated Ym1 and Ym2 crystals for comparison with *in vitro* generated recombinant Ym1 and Ym2 crystals.

Results

Recombinant Ym1 and Ym2 crystals are structurally similar to native crystals *ex vivo*

Individual crystals were harvested from the BAL fluid of me^v/me^v mice (carrying a defective protein tyrosine phosphatase SHP-1 gene) developing crystalline pneumonia [6] and C57BL/6J-Tg(CAG-Gal10)^{Bla} mice (transgenically overexpressing Gal10 from the ubiquitous CAG promotor, manuscript in preparation), sensitized and challenged with the allergen house dust mite (HDM). Crystallographic studies using microfocus synchrotron X-rays showed that the crystals obtained

from the BAL fluid of me^v/me^v mice were Ym1 crystals, in accordance with a previous report [6]. We had hypothesized that the crystals obtained from the BAL fluid of C57BL/6J-Tg(CAG-Gal10)^{Bla} mice were CLCs containing Gal10. However, crystallographic characterization of these crystals revealed that they are Ym2 crystals. In parallel, we produced recombinant Ym1 and Ym2 protein in FreeStyle 293-F cells. Spontaneous crystallization was aided by low pH and low temperature (4°C) (**Fig. 1 A, B**). Native *in vivo* isolated Ym1 crystals and recombinant Ym1 crystals (**Fig. 1 C**) as well as native *in vivo* isolated Ym2 crystals and recombinant Ym2 crystals (**Fig. 1 D**) were crystallographically equivalent, sharing the same monoclinic space group (P21) and unit-cell parameters. Moreover, X-ray crystallographic studies showed that a native *in vivo* isolated Ym1 crystal and a native *in vivo* isolated Ym2 crystal are structurally similar to each other, which is not so surprisingly as Ym1 (*Chil3*) and Ym2 (*Chil4*) are two closely related proteins sharing 95% nucleotide sequence identity and 91% amino acid sequence identity (**Fig. 1 E, F, G**). Crystallographic data and refinement statistics can be found in **Table S1**. Thus, recombinant Ym1 and Ym2 protein crystals can be generated *in vitro* and are biosimilar to native Ym1 and Ym2 crystals.

Ym1 crystals activate innate immunity

We next addressed whether Ym1 crystals could have pro-inflammatory effects in the lungs. Naïve WT C57BL/6 mice received an i.t. injection of 100 µg of endotoxin-low Ym1 crystals or control soluble Ym1 (**Fig. 2 A**). After 6 and 24 hours, there was a prominent influx of $Ly6C^+$ monocytes and eosinophils into the airways of mice receiving Ym1 crystals but not in those receiving soluble Ym1 or PBS. Neutrophil numbers were also increased in the Ym1 crystal group, but this failed to reach statistical significance (**Fig. 2 B**). This influx was accompanied by the production of the innate pro-inflammatory cytokines IL-6 and TNFα in BAL fluid (**Fig. 2 C**) and the inflammasome-dependent cytokine IL-1β and the alarmin IL-33 in lung tissue only in the group receiving crystalline Ym1 (**Fig. 2D**). Other cytokines like IL-1α and granulocyte-macrophage colony-stimulating factor (GM-CSF) were not consistently induced in any of the groups (data not shown). The monocyte chemoattractant CCL2 and the eosinophil chemoattractant CCL24 (Eotaxin-2) were found enhanced in lung tissue of the crystal-treated group (**Fig. 2 E**), particularly at early time points, suggesting these paracrine signals were driving the cellular influx induced by crystals.

As we were unable to make a crystallization-deficient soluble Ym1 mutein, we used WT soluble Ym1 protein as a control. However, we took into consideration that soluble Ym1 might crystallize *in vivo* after i.t. injection. To test this, we stained BAL pellets using a polyclonal anti Ym1/2 antibody and analyzed the samples using the ImageStream flow cytometry platform. The results clearly showed that the i.t. injected pre-formed Ym1 crystals were still present as intact crystals after 6 and 24 hours. The soluble Ym1 protein indeed crystallized *in vivo*, with crystals being clearly detectable after 6 hours and accumulating further after 24 hours. The crystals formed *in vivo* after i.t. injection of soluble Ym1 were also plate-like, but had a less uniform distribution and were smaller in size than the i.t. injected Ym1 crystals (**Fig. 2 F**). The total number of crystals found in the BAL pellet of soluble Ym1 treated mice (266 crystals in 5 pooled BAL pellets) was lower than in the BAL pellet of Ym1 crystal treated mice (1355 crystals in 5 pooled BAL pellets), potentially explaining why the soluble Ym1 group had less inflammation compared with the group receiving pre-formed Ym1 crystals.

Ym1 crystals activate DCs in the lymph nodes

We next studied whether innate immunity triggered by Ym1 crystals was accompanied by the induction of adaptive immunity, particularly since IL-1β, IL-33, IL-6 and TNFα in the lungs can activate antigen presenting cells [41]. Airway DCs bridge innate and adaptive immunity and can be activated by recombinant Gal10 crystals and monosodium urate (MSU) crystals [34,42]. Different subsets of DCs can be clearly distinguished from recruited monocytes and resident

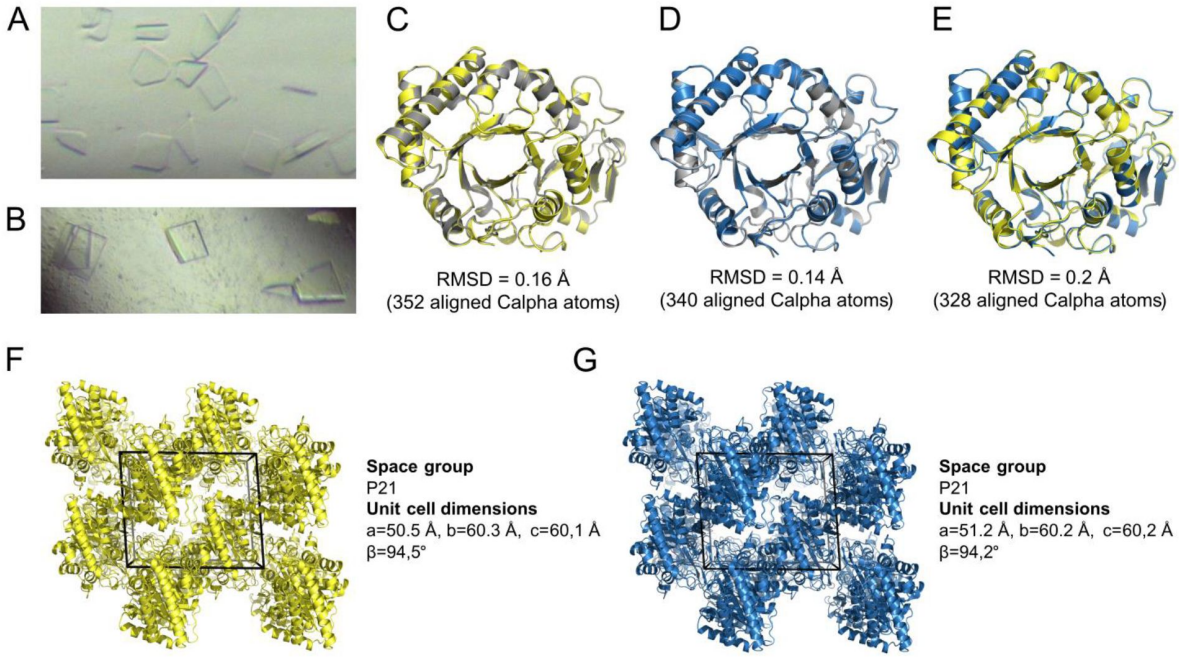

Figure 1

Recombinant Ym1 and Ym2 crystals are structurally similar to *in vivo* Ym1 and Ym2 crystals and to each other.

A, B) Light microscopy pictures of recombinant Ym1 (A) and Ym2 (B) crystals. **C-E)** Structural superposition of the X-ray structures determined from a native *in vivo* grown Ym1 crystal isolated from the BAL fluid of me^{v}/me^{v} mice (C+E) (yellow), a native *in vivo* grown Ym2 crystal isolated from the BAL fluid of a C57BL/6J-Tg(CAG-Gal10)^{Bla} mouse (D+E) (blue) and a recombinant Ym1 (C) and Ym2 (D) crystal (grey). The low root-mean-square deviations (RMSDs) establish structural similarity. **F, G)** Crystal packing of *ex vivo* Ym1 (F) and Ym2 (G) crystals revealing their crystallographic equivalence.

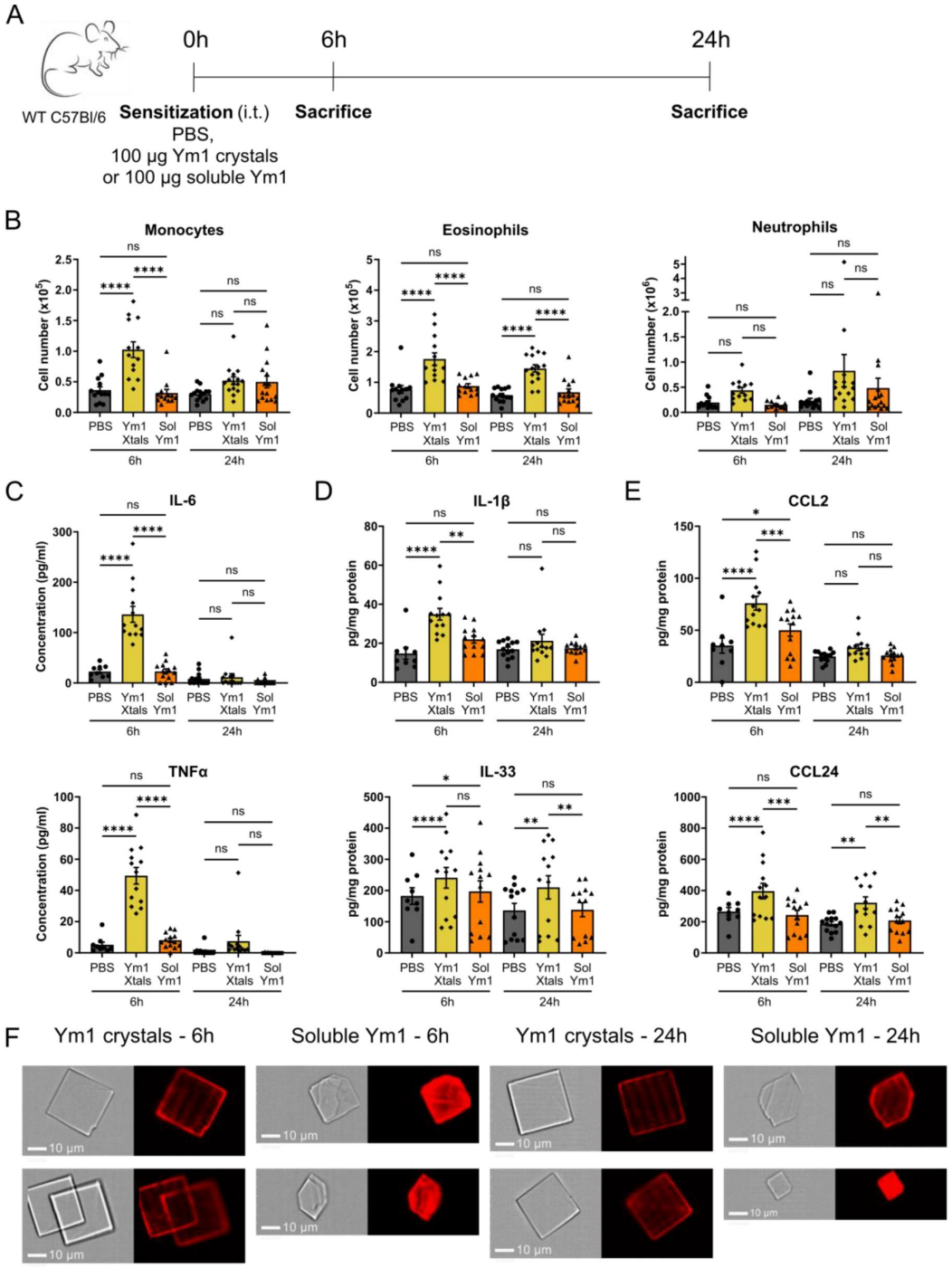

Figure 2

Ym1 crystals activate innate immunity.

A) Scheme representing the innate immune response experiment. **B)** Flow cytometric analysis of the immune cell influx in the lungs of PBS, Ym1 crystal and soluble Ym1 treated mice measured 6 and 24 hours after i.t. injection. Data are pooled from 2 (for 6h time point) or 3 (for 24h time point) independent experiments with n = 13, 13, 13, 14, 15 and 15, respectively. **C)** Concentration of IL-6 and TNFα in the BAL fluid measured by ELISA. **D, E)** Concentration of IL-1β, IL-33 (D), CCL2 and CCL24 (E) per milligram of protein of dispersed lung tissue measured by ELISA. Data are pooled from 2 independent experiments with n = 13 per group. Data are shown as mean ± SEM. ns P ≥ 0.05; *P < 0.05; **P<0,01; ***P <0.001; ****P < 0.0001. **F)** ImageStream pictures of the BAL fluid of Ym1 crystal and soluble Ym1 treated mice 6 and 24 hours after i.t. injection. Samples were stained with an antibody recognizing Ym1/2 (red).

macrophages based on the expression of CD26 and lack of expression of the complement C5a receptor CD88, and further separated into XCR1$^+$ cDC1 and CD172 (SIRPα)$^+$ cDC2 (see **Fig. 3A** for gating strategy) [30,43]. In mice given Ym1 crystals in the presence of fluorescently-labeled OVA antigen (**Fig. 3 B**), there was a clear increase in the number of total lung-draining mLN CD26$^+$CD88$^-$CD11c$^+$CD64$^-$ conventional DCs (cDCs), numerically mainly caused by an increase in the number of CD172$^+$ cDC2, compared with mice receiving PBS or soluble Ym1, although XCR1$^+$ cDC1s also clearly reacted to the crystals. There was also an increase in the number of mLN CD88$^+$CD11b$^+$ monocytes that expressed intermediate levels of CD11c induced by crystals (**Fig. 3 C**). Not surprisingly, the exposure to crystalline Ym1 also led to an increase in cDC1s, cDC2s and monocytes taking up the co-administered fluorescent OVA antigen (**Fig. 3 D**). Exposure to soluble Ym1 and Ym1 crystals also induced an upregulation of the costimulatory molecules CD80 (data not shown) and CD86, and this effect was most pronounced with crystalline Ym1, and particularly in cDCs that were also taking up fluorescent OVA (**Fig. 3 E**).

Ym1 crystals boost adaptive type 2 immunity

We next asked whether crystalline or soluble Ym1 could boost adaptive cellular immunity to co-administered OVA, when DCs that have taken up antigen and matured migrate to mLNs (**Fig. 4 A**). To evaluate induction of type 2 immunity in naïve antigen-specific T cells directly, cell tracer violet labeled OVA-reactive CD4$^+$ T cell receptor (TCR) MHCII-restricted transgenic T cells (OT-II T cells) crossed to the huCD2-IL-4 (KN2) reporter strain were transferred into WT mice, allowing us to track T cell division simultaneously with the acquisition of a Th2-polarized state *in vivo* [44]. When innocuous OVA was injected i.t. together with Ym1 crystals, the adoptively transferred OT-II KN2 T cells showed increased proliferation 4 days (**Fig. 4 B**) and 7 days (data not shown) later in the mLNs, an effect absent when OVA was given with soluble Ym1. This led to the accumulation of higher numbers of OT-II T cells and Th2 polarizing KN2+ OT-II T cells in the mLNs 4 days (**Fig. 4 C**) and 7 days (**Fig. 4 D**) after the i.t. administration. After 7 days, divided OT-II T cells and KN2+ OT-II T cells could also be found in the lungs of mice receiving OVA mixed with Ym1 crystals (**Fig. 4 E**). These cells lost CD62L expression while expressing CD44, showing they had become effector cells (data not shown). These effects on T cell activation and Th2 polarization were again not observed when OVA was injected together with soluble Ym1. Early IL-4 production in OVA-reactive OT-II cells could also point to differentiation of T cells into T follicular helper (T_{FH}) cells that provide help for germinal center reactions. However, we did not add CXCR5 or PD1 to study T_{FH} development in greater detail.

We finally tested whether Ym1 crystals could also promote allergic type 2 inflammation to inhaled harmless antigens, typically observed in asthmatics. WT C57BL/6 mice were sensitized i.t. with OVA mixed with Ym1 crystals on days 0 and 1 and received OVA i.n. challenges on days 11 to 13 (**Fig. 5 A**). These mice exhibited airway inflammation characterized by an influx of eosinophils, B cells and T cells (**Fig. 5 B**), a higher production of the type 2 cytokines IL-5, IL-10 and IL-13 in the supernatants of mLN restimulation cultures (**Fig. 5 C**) and a robust OVA-specific IgG1 response, a hallmark of type 2 immunity, most likely driven by enhanced IL-4 production in Th2 or T_{FH} cells (**Fig. 5 D**). These effects were not observed when OVA alone was used as the immunogen or when OVA was co-administered with soluble Ym1. Thus, the induction of allergic type 2 inflammation was specifically related to the crystalline state of Ym1. In contrast to recombinant Gal10 crystals, which mounted high titers of Gal10-specific IgG1 antibodies when used as adjuvant in the same experimental set-up [34], Ym1 crystals did not elicit an antibody response directed to Ym1 (**Fig. 5 E**). However, when mice received repetitive injections of Ym1 crystals in a different set-up via i.p. injection (**Fig. 5 F**), high titers of Ym1-specific IgM were detected (**Fig. 5 G**), suggesting that Ym1 crystals can trigger an auto-immune response or elicit a recall response from natural IgM antibody producing peritoneal B cells.

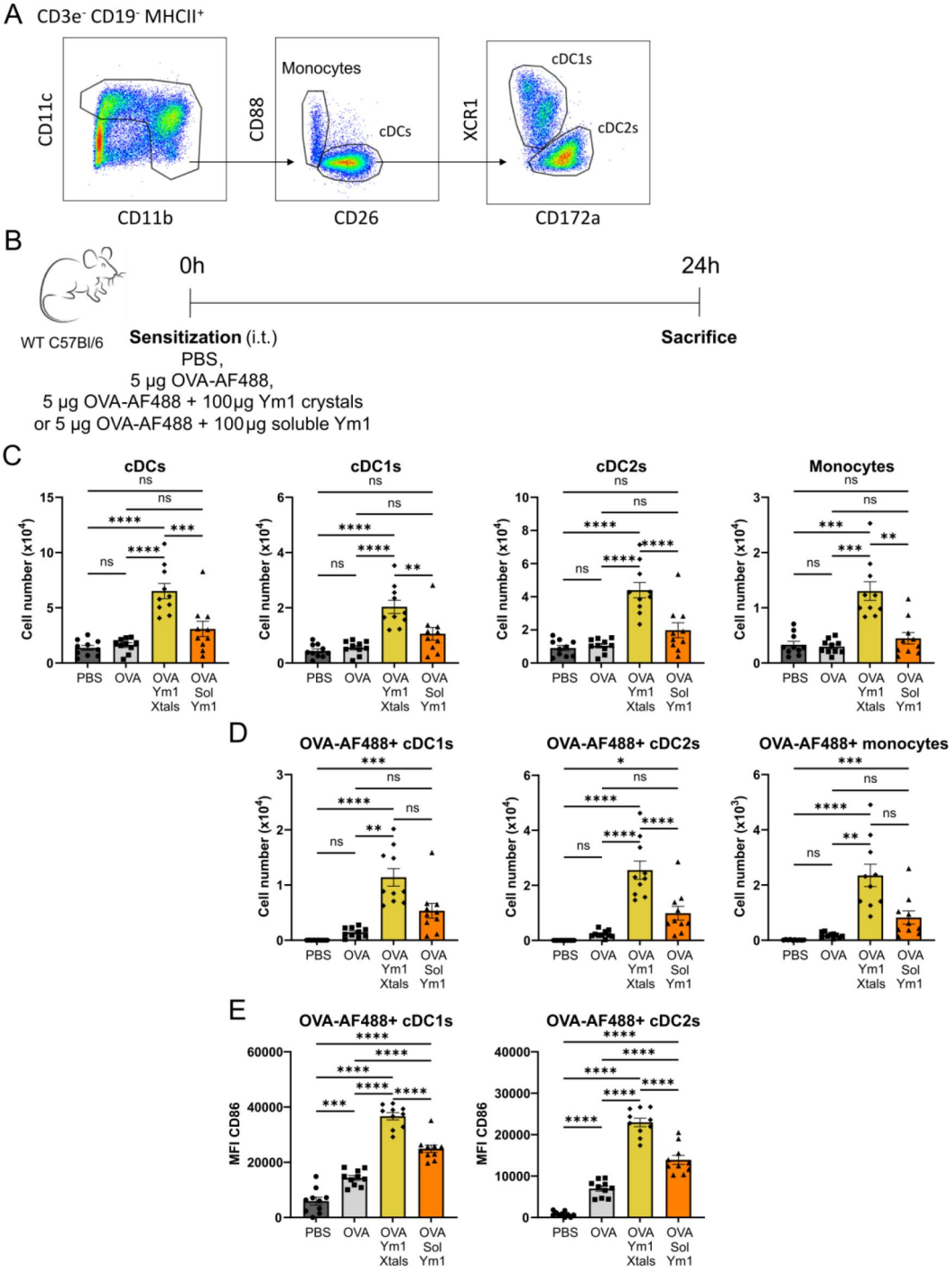

Figure 3

Ym1 crystals activate DCs in the lymph nodes.

A) Gating strategy to distinguish different subsets of DCs and recruited monocytes. **B)** Scheme representing the DC activation experiment. **C, D)** Flow cytometric analysis of the DC and monocyte influx in the mLNs of PBS, OVA-AF488 alone, OVA-AF488 plus Ym1 crystals and OVA-AF488 plus soluble Ym1 treated mice measured 24 hours after i.t. injection. **E)** Median Fluorescence Intensity (MFI) of activation marker CD86 on OVA-AF488+ cDC1s and cDC2s of PBS, OVA-AF488 alone, OVA-AF488 plus Ym1 crystals and OVA-AF488 plus soluble Ym1 treated mice measured 24 hours after i.t. injection. Data are pooled from 2 independent experiments with n = 10 mice per group. Data are shown as mean ± SEM. ns P ≥ 0.05; *P < 0.05; **P<0,01; ***P <0.001; ****P < 0.0001.

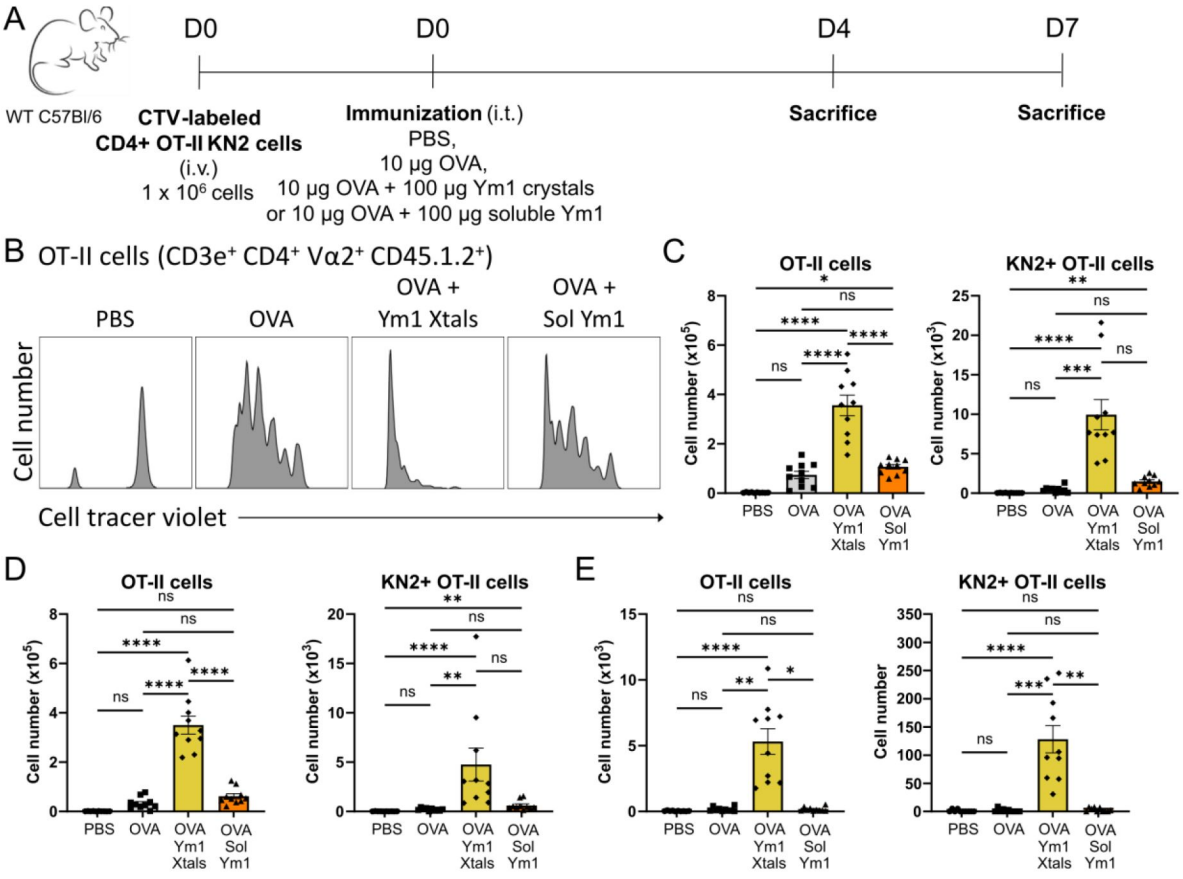

Figure 4

Ym1 crystals boost adaptive cellular immunity.

A) Scheme representing the used adoptive transfer model. **B-E)** Proliferation and KN2 expression of OT-II T cells in the mLNs and lungs 4 and 7 days after i.t. administration of PBS, OVA alone, OVA plus Ym1 crystals or OVA plus soluble Ym1. (B) Representative histograms of the division profile of the adoptively transferred OT-II T cells ($CD3e^+$ $CD4^+$ $V\alpha2^+$ $CD45.1.2^+$) in the mLNs on day 4. (C, D) The numbers of OT-II T cells and KN2+ OT-II T cells in the mLNs on day 4 (C) and day 7 (D). (E) The numbers of OT-II T cells and KN2+ OT-II T cells in the lungs on day 7. Data are pooled from 2 independent experiments with n = 10 mice per group. Data are shown as mean ± SEM. ns $P \geq 0.05$; *$P < 0.05$; **P<0,01; ***P <0.001; ****$P < 0.0001$.

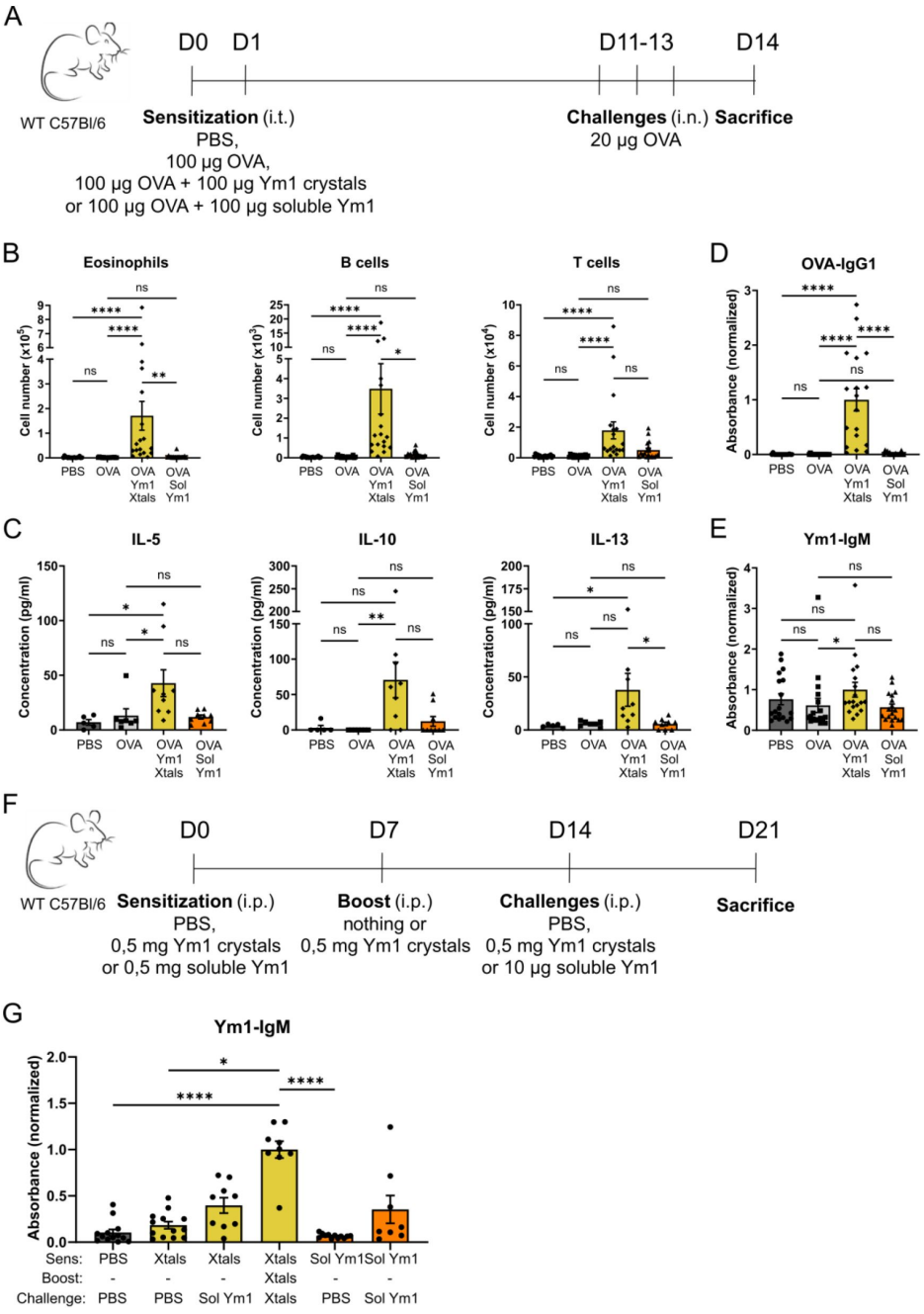

Figure 5

Ym1 crystals can act as type 2 adjuvant in OVA-induced asthma model and activate adaptive humoral immunity.

A) Scheme representing the used OVA-induced asthma model. **B)** Flow cytometric analysis of the immune cell influx in the BAL fluid of mice sensitized i.t. with PBS, OVA alone, OVA plus Ym1 crystals or OVA plus soluble Ym1 and challenged i.n. with OVA. Data are pooled from 2 independent experiments with n = 18 per group. **C)** Levels of IL-5, IL-10 and IL-13 in the supernatant of mLN cells after restimulation with OVA for 20 hours. Data are from 1 experiment with n = 5, 7, 9 and 9, respectively. **D)** Serum OVA-specific IgG1 antibodies were measured by ELISA. **E)** Serum Ym1-specific IgM antibodies were measured by ELISA. Data are pooled from 2 independent experiments with n = 18 per group. **F)** Scheme representing the adaptive humoral immune response experiment. **G)** Serum Ym1-specific IgM antibodies were measured by ELISA. Data are pooled from 3 independent experiments with n = 13, 13, 9, 9, 12 and 8, respectively. Data are shown as mean ± SEM. ns P ≥ 0.05; *P < 0.05; **P<0,01; ****P < 0.0001. If pairwise comparison is not shown, the result is not significant.

Discussion

Ym1 and Ym2 are among the most strongly induced proteins in the airways of mice after allergen exposure[45,49] and both proteins readily form pseudo-CLCs *in vivo*. As a result, Ym1 and Ym2 have become markers of type 2 inflammation. Here we show by *ex vivo* X-ray crystallography that Ym2 also crystallizes *in vivo* and that the phase transition of soluble Ym1/Ym2 to crystalline pseudo-CLC states leads to profound immunostimulatory effects on innate and adaptive type 2 immunity. Sutherland and colleagues have shown that vector-based overexpression of Ym1 or Ym2 in the lung increased the number of neutrophils in the BAL fluid [50]. Whether these observed effects were due to the crystalline or soluble state of Ym1/2 remains unclear from these studies. Also in the present study, we lacked a proper soluble Ym1 control, since ImageStream analysis showed the soluble Ym1 protein to readily crystallize upon injection in the lungs. So far, several attempts to produce crystallization-deficient soluble Ym1 or Ym2 muteins failed, despite the fact that this was feasible for the CLC protein Gal10 [34]. In Persson *et al.* (2019), we produced anti-Gal10 antibodies able to dissolve pre-existing CLCs and to inhibit key features of airway CLC crystallopathy in a humanized mouse model of asthma [34]. Sutherland and colleagues have shown that blocking antibodies directed against Ym1/2 suppressed neutrophilic inflammation in the lungs of asthmatic mice and helminth-infected mice [34,50]. However, it is unclear if these anti-Ym1/2 antibodies used suppressed lung neutrophilia by dissolving possible Ym1/2 pseudo-CLCs. We also observed that Ym1 crystals induced an auto-antibody response of the IgM isotype, suggesting intrinsic adjuvant activity in the crystalline state of Ym1. Antibodies to Ym1/2 have been described to occur also in a model of incipient neoplasia in mice overexpressing the Epstein Barr virus oncogene LMP1 in the skin, leading to chronic inflammation[51]. However, it is unclear if induction of such auto-antibodies to Ym1/2 would be the result of spontaneous crystallization of Ym1/2 in the skin of these mice. Recognition of endogenously produced MSU or cholesterol crystals by IgM has been described previously [52,53], and in the case of MSU, it was even proposed that IgM is required to turn soluble uric acid (UA) into an immunostimulatory adjuvant [53]. Future studies will have to establish if IgM contributes in some way to the adjuvanticity of Ym1 crystals or facilitates the transition of soluble to crystalline Ym1.

Ym1 (*Chil3*) and Ym2 (*Chil4*) share 95% nucleotide sequence identity and 91% amino acid sequence identity and we now show here that native *in vivo* grown Ym1 crystals are structurally similar to native *in vivo* grown Ym2 crystals. Given these similarities, we assume that Ym2 crystals most likely will stimulate innate and adaptive immunity and act as a type 2 adjuvant, similar to Ym1 crystals, although we did not formally demonstrate this experimentally. We can only speculate why, from an evolutionary perspective, mice even express two very similar proteins that are expressed under similar conditions and share the peculiar property to crystalize *in vivo*. However, Ym1 is mainly expressed by macrophages, neutrophils and a subset of circulating pro-repair monocytes, while Ym2 is produced by lung epithelial cells, which could have discrete context dependent benefits. We have also not formally proven that Ym2 crystals have the same immunostimulatory effects on type 2 immunity as Ym1 crystals, but based on structural homology, we propose they do. Also, future studies will have to elucidate if soluble Ym1 and Ym2 have similar effects on immunity and tissue remodeling. A phase transition to its crystalline state may therefore mean different things for Ym1 and Ym2 biology *in vivo*.

Understanding the requirements for protein crystal formation during type 2 immunity, studying the mechanisms whereby protein crystals stimulate type 2 immunity and having the proper tools to be able to distinguish between the soluble and the crystalline state will help us to better understand if targeting CLCs in human asthma and chronic rhinosinusitis with nasal polyps (CRSwNPs) would be of value. Since CLCs and pseudo-CLCs are almost exclusively found in eosinophilic airway inflammation across many species, and share many biological effects, it appears that protein crystallization is a more generalized feature of type 2 immunity. The cellular influx and production of several cytokines and chemokines we observed after recombinant Ym1 crystal injection was also observed in earlier work where recombinant Gal10 crystals were

injected into the lung of mice [34]. Besides triggering innate immunity, Gal10 crystals, just like Ym1 crystals were able to recruit and activate DCs, activate cellular and humoral adaptive immune responses and act as type 2 adjuvants [34]. Besides, not only protein crystals, but also organic non-proteinaceous crystals such as MSU crystals and crystalline alum were able to recruit and activate DCs and act as type 2 adjuvants [42,54], suggesting that promotion of type 2 response is a generic response to crystals of different chemical composition. The convergent evolution of CLCs and pseudo-CLCs as protein crystals in type 2 immunity strongly suggests a selective evolutionary advantage of these protein crystals in the enhancement of type 2-driven immune responses.

Acknowledgements

We acknowledge the crucial help of the staff of the VIB Protein Synthesis Core, the VIB Flow Cytometry core, the VIB Bioimaging core, and. S.N.S., K.V., and K.H.G.V. thank the staff and management of synchrotron beamlines P14 (PETRA 3, Hamburg, Germany), Proxima 1 (SOLEIL, Saclay, France), and PX1 (Swiss Light Source, Villigen, Switzerland) for beamtime allocation and support during data collection of X-ray diffraction data.

B.N.L. acknowledges support from ERC advanced grant (789384 ASTHMA CRYSTAL CLEAR), a concerted research initiative grant from Ghent University (GOA, 01G010C9), an FWO Methusalem grant (01M01521) and an FWO EOS research grant (3G0H1222), and the Flanders Institute of Biotechnology (VIB). S.N.S. acknowledges support to this project from the Ghent University GOA program (BOF17-GOA-028).

Protein complex	Recombinant Ym1	*Ex vivo* Ym1	Recombinant Ym2	*Ex vivo* Ym2
Data collection				
X-ray source (beamline)	SOLEIL (Proxima 1)	PETRA III (P14)	PETRA III (P14)	SLS (PXI)
Wavelength (Å)	0.97857	0.9763	0.9763	1.0000089224
Space group	*P21*	*P21*	*P21*	*P21*
Cell dimensions				
a, *b*, *c* (Å)	50.33, 60.01, 60.12	50.52, 60.25, 60.12	51.09, 59.90, 59.88	51.26, 60.21, 60.17
α, β, γ (°)	90.00, 94.66, 90.00	90.00, 94.48, 90.00	90.00, 94.14, 90.00	90.00, 94.24, 90.00
Resolution (Å)	50.00-1.79 (1.90-1.79)	59.93-1.42 (1.50-1.42)	59.90-1.17 (1.24-1.17)	42.50-1.70 (1.81-1.70)
R_{meas} (%)	24.7 (112.1)	12.2 (138.2)	8.0 (35.8)	17.7 (136.4)
$< I/\sigma >$	5.28 (1.54)	8.99 (1.19)	15.12 (4.74)	6.59 (0.96)
CC ½ (%)	97.9 (56.6)	99.7 (39.5)	99.9 (92.5)	99.2 (35.8)
Completeness (%)	99.2 (96.0)	98.1 (97.3)	98.4 (95.9)	97.7 (97.3)
Redundancy	4.1 (3.9)	3.3 (3.3)	6.8 (6.1)	3.5 (3.4)
ISa score	8.04	26.18	27.31	24.20
Wilson B ($Å^2$)	20.318	20.936	12.048	24.584
Refinement				
Resolution (Å)	42.40-1.79	26.91-1.42	37.45-1.17	16.78-1.71
No. reflections	33 407	66 944	119 181	39 026
R_{work} / R_{free} (%)	17.29 / 19.86	18.10 / 20.52	15.75 / 16.73	17.71 / 20.48
No. non-H atoms				
Protein	2 957	2 957	2 976	2 970
Ligand/ion	10	4	24	6
Water	215	163	584	239
B-factors ($Å^2$)				
Protein	12.09	15.58	10.28	18.50
Ligand/ion	21.52	30.73	16.20	30.69
Water	21.74	22.78	27.02	27.93
R.m.s. deviations				
Bond lengths (Å)	0.008	0.010	0.010	0.010
Bond angles (°)	0.91	0.98	1.07	0.97

§Each dataset was collected from a single crystal. *Values in parentheses are for highest-resolution shell.

Table S1.

Crystallographic data and refinement statistics§,*

References

1. Charcot J., Vulpian A. (1860) **Note sur des cristaux particuliers trouvés dans le sang et dans certains viscèresd'un sujet leucémique, et sur d'autres faits necroscopiques observés sur le même sujet** *Gaz. Hebd. de Méd et Chirurgie* :755–758

2. von Leyden E. (1872) **Zur Kenntniss des bronchial asthma. (Virchov)** *Arch. Pathol. Anat* **54**:324–344

3. Aegerter H., et al. (2021) **Charcot-Leyden crystals and other protein crystals driving type 2 immunity and allergy** *Curr Opin Immunol* **72**:72–78

4. Doye J.P., Louis A.A., Vendruscolo M. (2004) **Inhibition of protein crystallization by evolutionary negative design** *Phys Biol* **1**:P9–13

5. Schönherr R., Rudolph J.M., Redecke L. (2018) **Protein crystallization in living cells** *Biol Chem* **399**:751–772

6. Guo L., Johnson R.S., Schuh J.C. (2000) **Biochemical characterization of endogenously formed eosinophilic crystals in the lungs of mice** *J Biol Chem* **275**:8032–8037

7. Hoenerhoff M.J., Starost M.F., Ward J.M. (2006) **Eosinophilic crystalline pneumonia as a major cause of death in 129S4/SvJae mice** *Vet Pathol* **43**:682–688

8. Takamoto M., et al. (1997) **Eosinophilia, parasite burden and lung damage in Toxocara canis infection in C57Bl/6 mice genetically deficient in IL-5** *Immunology* **90**:511–517

9. Shultz L.D., Coman D.R., Bailey C.L., Beamer W.G., Sidman C.L. (1984) **"Viable motheaten," a new allele at the motheaten locus. I. Pathology** *Am J Pathol* **116**:179–192

10. Harbord M., et al. (2002) **Ym1 is a neutrophil granule protein that crystallizes in p47phox-deficient mice** *J Biol Chem* **277**:5468–5475

11. Liu Q., et al. (2009) **p47phox deficiency induces macrophage dysfunction resulting in progressive crystalline macrophage pneumonia** *Am J Pathol* **174**:153–163

12. Waern I., et al. (2010) **Accumulation of Ym1 and formation of intracellular crystalline bodies in alveolar macrophages lacking heparanase** *Mol Immunol* **47**:1467–1475

13. Poczobutt J.M., et al. (2021) **Altered Macrophage Function Associated with Crystalline Lung Inflammation in Acid Sphingomyelinase Deficiency** *Am J Respir Cell Mol Biol* **64**:629–640

14. Fallon P.G., Emson C.L., Smith P., McKenzie A.N. (2001) **IL-13 overexpression predisposes to anaphylaxis following antigen sensitization** *J. Immunol* **166**:2712–2716

15. Rehm S., Wcislo A., Deerberg F. (1985) **Non-neoplastic lesions of female virgin Han:NMRI mice, incidence and influence of food restriction throughout life span. II: Respiratory tract** *Lab Anim* **19**:224–235

16. Green E. (1942) **On the occurrence of crystalline material in the lungs of normal and cancerous Swiss mice** *Cancer Res* **2**:210–217

17. Murray A.B., Luz A. (1990) **Acidophilic macrophage pneumonia in laboratory mice** *Vet Pathol* **27**:274–281

18. Yang Y.H., Campbell J.S. (1964) **Crystalline excrements in bronchitis and cholecystitis of mice** *Am J Pathol* **45**:337–345

19. Feldmesser M., Kress Y., Casadevall A. (2001) **Intracellular crystal formation as a mechanism of cytotoxicity in murine pulmonary Cryptococcus neoformans infection** *Infect Immun* **69**:2723–2727

20. Baldán A., Gomes A.V., Ping P., Edwards P.A. (2008) **Loss of ABCG1 results in chronic pulmonary inflammation** *J Immunol* **180**:3560–3568

21. Huffnagle G.B., Boyd M.B., Street N.E., Lipscomb M.F. (1998) **IL-5 is required for eosinophil recruitment, crystal deposition, and mononuclear cell recruitment during a pulmonary Cryptococcus neoformans infection in genetically susceptible mice (C57BL/6)** *J. Immunol* **160**:2393–2400

22. Mall M.A., et al. (2008) **Development of chronic bronchitis and emphysema in beta-epithelial Na+ channel-overexpressing mice** *Am J Respir Crit Care Med* **177**:730–742

23. Roediger B., et al. (2015) **IL-2 is a critical regulator of group 2 innate lymphoid cell function during pulmonary inflammation** *J Allergy Clin Immunol* **136**:1653–1663

24. Henderson W.R., et al. (2002) **A role for cysteinyl leukotrienes in airway remodeling in a mouse asthma model** *Am J Respir Crit Care Med* **165**:108–116

25. Zhu Z., et al. (1999) **Pulmonary expression of interleukin-13 causes inflammation, mucus hypersecretion, subepithelial fibrosis, physiologic abnormalities, and eotaxin production** *J Clin Invest* **103**:779–788

26. Leonidas D.D., et al. (1995) **Crystal structure of human Charcot-Leyden crystal protein, an eosinophil lysophospholipase, identifies it as a new member of the carbohydrate-binding family of galectins** *Structure* **3**:1379–1393

27. Swaminathan G.J., Leonidas D.D., Savage M.P., Ackerman S.J., Acharya K.R. (1999) **Selective recognition of mannose by the human eosinophil Charcot-Leyden crystal protein (galectin-10): a crystallographic study at 1.8 A resolution** *Biochemistry* **38**:13837–13843

28. Raes G., et al. (2002) **Differential expression of FIZZ1 and Ym1 in alternatively versus classically activated macrophages** *J Leukoc Biol* **71**:597–602

29. Ikeda N., et al. (2018) **Emergence of immunoregulatory Ym1(+)Ly6C(hi) monocytes during recovery phase of tissue injury** *Sci Immunol* **3**

30. Aegerter H., Lambrecht B.N., Jakubzick C.V. (2022) **Biology of lung macrophages in health and disease** *Immunity* **55**:1564–1580

31. Ward J.M., et al. (2001) **Hyalinosis and Ym1/Ym2 gene expression in the stomach and respiratory tract of 129S4/SvJae and wild-type and CYP1A2-null B6, 129 mice** *Am J Pathol* **158**:323–332

32. Parkinson J.E., Pearson S., Rückerl D., Allen J.E., Sutherland T.E. (2021) **The magnitude of airway remodeling is not altered by distinct allergic inflammatory responses in BALB/c versus C57BL/6 mice but matrix composition differs** *Immunol Cell Biol* **99**:640–655

33. Van Dyken S.J., Locksley R.M. (2018) **Chitins and chitinase activity in airway diseases** *J Allergy Clin Immunol* **142**:364–369

34. Persson E.K., et al. (2019) **Protein crystallization promotes type 2 immunity and is reversible by antibody treatment** *Science* **364** https://doi.org/10.1126/science.aaw4295

35. Kabsch W. (2010) **Integration, scaling, space-group assignment and post-refinement** *Acta Crystallogr D Biol Crystallogr* **66**:133–144

36. Winn M.D., et al. (2011) **Overview of the CCP4 suite and current developments** *Acta Crystallogr D Biol Crystallogr* **67**:235–242

37. McCoy A.J., et al. (2007) **Phaser crystallographic software** *J Appl Crystallogr* **40**:658–674

38. Emsley P., Lohkamp B., Scott W.G., Cowtan K. (2010) **Features and development of Coot** *Acta Crystallographica Section D: Biological Crystallography* **66**:486–501

39. Bricogne G. B.E., Brandl M., Flensburg C., Keller P., Paciorek W., Roversi P S.A., Smart O.S., Vonrhein C., Womack T.O. (2017) **BUSTER version 2.10.3**

40. Joosten R.P., Long F., Murshudov G.N., Perrakis A. (2014) **The PDB_REDO server for macromolecular structure model optimization** *IUCrJ* **1**:213–220

41. Lambrecht B.N., Hammad H. (2012) **Lung dendritic cells in respiratory viral infection and asthma: from protection to immunopathology** *Annu Rev Immunol* **30**:243–270

42. Kool M., et al. (2011) **An unexpected role for uric acid as an inducer of T helper 2 cell immunity to inhaled antigens and inflammatory mediator of allergic asthma** *Immunity* **34**:527–540

43. Rawat K., et al. (2023) **CCL5-producing migratory dendritic cells guide CCR5+ monocytes into the draining lymph nodes** *J Exp Med* **220**

44. Mohrs M., Shinkai K., Mohrs K., Locksley R. (2001) **Analysis of type 2 immunity in vivo with a bicistronic reporter** *Immunity* **15**:303–311

45. Jeong H., et al. (2005) **Proteomic analysis of differently expressed proteins in a mouse model for allergic asthma** *J Korean Med Sci* **20**:579–585

46. Zhao J., Zhu H., Wong C.H., Leung K.Y., Wong W.S. (2005) **Increased lungkine and chitinase levels in allergic airway inflammation: a proteomics approach** *Proteomics* **5**:2799–2807

47. Zhao J., Yeong L.H., Wong W.S. (2007) **Dexamethasone alters bronchoalveolar lavage fluid proteome in a mouse asthma model** *Int Arch Allergy Immunol* **142**:219–229

48. Wong W.S., Zhu H., Liao W. (2007) **Cysteinyl leukotriene receptor antagonist MK-571 alters bronchoalveolar lavage fluid proteome in a mouse asthma model** *Eur J Pharmacol* **575**:134–141

49. Wong W.S., Zhao J. (2008) **Proteome analysis of chronically inflamed lungs in a mouse chronic asthma model** *Int Arch Allergy Immunol* **147**:179–189

50. Sutherland T.E., et al. (2014) **Chitinase-like proteins promote IL-17-mediated neutrophilia in a tradeoff between nematode killing and host damage** *Nat Immunol* **15**:1116–1125

51. Qureshi A.M., Hannigan A., Campbell D., Nixon C., Wilson J.B. (2011) **Chitinase-like proteins are autoantigens in a model of inflammation-promoted incipient neoplasia** *Genes Cancer* **2**:74–87

52. Pilely K., et al. (2016) **Cholesterol Crystals Activate the Lectin Complement Pathway via Ficolin-2 and Mannose-Binding Lectin: Implications for the Progression of Atherosclerosis** *J Immunol* **196**:5064–5074

53. Kanevets U., Sharma K., Dresser K., Shi Y. (2009) **A role of IgM antibodies in monosodium urate crystal formation and associated adjuvanticity** *J Immunol* **182**:1912–1918

54. Williams G.R., et al. (2014) **Immunity induced by a broad class of inorganic crystalline materials is directly controlled by their chemistry** *J Exp Med* **211**:1019–1025

Article and author information

Ines Heyndrickx
Laboratory of Immunoregulation and Mucosal Immunology, VIB-UGent Center for Inflammation Research, Ghent, Belgium, Department of Internal Medicine and Pediatrics, Ghent University, Ghent, Belgium
ORCID iD: 0000-0001-8091-6390

Kim Deswarte
Laboratory of Immunoregulation and Mucosal Immunology, VIB-UGent Center for Inflammation Research, Ghent, Belgium, Department of Internal Medicine and Pediatrics, Ghent University, Ghent, Belgium
ORCID iD: 0000-0002-9761-6973

Kenneth Verstraete
Unit for Structural Biology, VIB-UGent Center for Inflammation Research, Ghent, Belgium, Department of Biochemistry and Microbiology, Ghent University, Ghent, Belgium
ORCID iD: 0000-0001-6544-6458

Koen H. G. Verschueren
Unit for Structural Biology, VIB-UGent Center for Inflammation Research, Ghent, Belgium, Department of Biochemistry and Microbiology, Ghent University, Ghent, Belgium
ORCID iD: 0000-0002-3522-9169

Ursula Smole
Laboratory of Immunoregulation and Mucosal Immunology, VIB-UGent Center for Inflammation Research, Ghent, Belgium, Department of Internal Medicine and Pediatrics, Ghent University, Ghent, Belgium
ORCID iD: 0000-0001-5124-2024

Helena Aegerter
Laboratory of Immunoregulation and Mucosal Immunology, VIB-UGent Center for Inflammation Research, Ghent, Belgium, Department of Internal Medicine and Pediatrics, Ghent University, Ghent, Belgium
ORCID iD: 0000-0002-5755-9126

Ann Dansercoer
Unit for Structural Biology, VIB-UGent Center for Inflammation Research, Ghent, Belgium, Department of Biochemistry and Microbiology, Ghent University, Ghent, Belgium
ORCID iD: 0000-0002-8689-3887

Hamida Hammad
Laboratory of Immunoregulation and Mucosal Immunology, VIB-UGent Center for Inflammation Research, Ghent, Belgium, Department of Internal Medicine and Pediatrics, Ghent University, Ghent, Belgium
ORCID iD: 0000-0003-3762-8603

Savvas N. Savvides
Unit for Structural Biology, VIB-UGent Center for Inflammation Research, Ghent, Belgium, Department of Biochemistry and Microbiology, Ghent University, Ghent, Belgium
ORCID iD: 0000-0003-3420-5947

Bart N. Lambrecht
Laboratory of Immunoregulation and Mucosal Immunology, VIB-UGent Center for Inflammation Research, Ghent, Belgium, Department of Internal Medicine and Pediatrics, Ghent University, Ghent, Belgium, Department of Pulmonary Medicine, Erasmus University Medical Center Rotterdam, Rotterdam, The Netherlands
For correspondence: Bart.Lambrecht@ugent.be
ORCID iD: 0000-0003-4376-6834

Copyright

Editors

Reviewing Editor
Florent Ginhoux
Agency for Science Technology and Research, Singapore, Singapore

Senior Editor
Tadatsugu Taniguchi
University of Tokyo, Tokyo, Japan

Reviewer #1 (Public Review):

Summary:

The manuscript by Heyndrickx et al describes protein crystal formation and function that bears similarity to Charcot-Leyden crystals made of galectin 10, found in humans under similar conditions. Therefore, the authors set out to investigate CLP crystal formation and their immunological effects in the lung. The authors reveal the crystal structure of both Ym1 and Ym2 and show that Ym1 crystals trigger innate immunity, activated dendritic cells in the lymph node, enhancing antigen uptake and migration to the lung, ultimately leading to induction of type 2 immunity.

Strengths:

We know a lot about expression levels of CLPs in various settings in the mouse, but still know very little about the functions of these proteins, especially in light of their ability to form crystal structures. As such data presented in this paper is a major advance to the field.

Resolving the crystal structure of Ym2 and the comparison between native and recombinant CLP crystals is a strength of this manuscript that will be a very powerful tool for further evaluation and understanding of receptor, binding partner studies including ability to aid mutant protein generation.

The ability to recombinantly generate CLP crystals and study their function in vivo and ex vivo has provided a robust dataset whereby CLPs can activate innate immune responses, aid activation and trafficking of antigen presenting cells from the lymph node to the lung and further enhances type 2 immunity. By demonstrating these effects the authors directly address the aims for the study. A key apoint of this study is the generation of a model in which crystal formation/function an important feature of human eosinophilic diseases, can be studied utilising mouse models. Excitingly, using crystal structures combined with understanding the biochemistry of these proteins will provide a potential avenue whereby inhibitors could be used to dissolve or prevent crystal formation in vivo.

Generation of the crystal structure for Ym2 is a particular strength of the authors work and highlights the similarities between Ym1 and Ym2. Whilst the authors did not specifically examine Ym2 function, they have provided a discussion on this and speculate that Ym2 will function in a similar manner to Ym1.

The data presented flows logically and formulates a well constructed overall picture of exactly what CLP crystals could be doing in an inflammatory setting in vivo. Leaves open a clear and exciting future avenue (currently beyond the scope of this work) for determining whether targeting crystal formation in vivo could limit pathology.

Weaknesses:

It would have been nice for the authors to confirm whether Ym2 has similar functions to Ym1 using the in vivo and in vitro systems. However, they have discussed these points and raised it as a potential for future studies.

- https://doi.org/10.7554/eLife.90676.2.sa1

Reviewer #2 (Public Review):

Summary:

This interesting study addresses the ability of Ym1 protein crystals to promote pulmonary type 2 inflammation in vivo, in mice.

Strengths:

The data are extremely high quality, clearly presented, significantly extending previous work from this group on the type 2 immunogenicity of protein crystals.

Weaknesses:

There are no major weaknesses in this study. It would be interesting to see if Ym2 crystals behave similarly to Ym1 crystals in vivo. Some additional text in the Introduction and Discussion would enrich those sections.

- https://doi.org/10.7554/eLife.90676.2.sa0

Author Response

The following is the authors' response to the original reviews.

> ***Public Reviews:***
>
> ***Reviewer #1 (Public Review):***
>
> *Summary:*
>
> *The manuscript by Heyndrickx et al describes protein crystal formation and function that bears similarity to Charcot-Leyden crystals made of galectin 10, found in humans under similar conditions. Therefore, the authors set out to investigate CLP crystal formation and their immunological effects in the lung. The authors reveal the crystal structure of both Ym1 and Ym2 and show that Ym1 crystals trigger innate immunity, activated dendritic cells in the lymph node, enhancing antigen uptake and migration to the lung, ultimately leading to induction of type 2 immunity.*
>
> *Strengths:*
>
> *We know a lot about expression levels of CLPs in various settings in the mouse but still know very little about the functions of these proteins, especially in light of their ability to form crystal structures. As such data presented in this paper is a major advance to the field.*
>
> *Resolving the crystal structure of Ym2 and the comparison between native and recombinant CLP crystals is a strength of this manuscript that will be a very powerful tool for further evaluation and understanding of receptor, binding partner studies including the ability to aid mutant protein generation.*
>
> *The ability to recombinantly generate CLP crystals and study their function in vivo and ex vivo has provided a robust dataset whereby CLPs can activate innate immune responses, aid activation and trafficking of antigen presenting cells from the lymph node to the lung and further enhances type 2 immunity. By demonstrating these effects the authors directly address the aims for the study. A key point of this study is the generation of a model in which crystal formation/function an important feature of human eosinophilic diseases, can be studied utilising mouse models. Excitingly, using crystal structures combined with understanding the biochemistry of these proteins will provide a potential avenue whereby inhibitors could be used to dissolve or prevent crystal formation in vivo.*
>
> *The data presented flows logically and formulates a well constructed overall picture of exactly what CLP crystals could be doing in an inflammatory setting in vivo. This leaves open a clear and exciting future avenue (currently beyond the scope of this work) for determining whether targeting crystal formation in vivo could limit pathology.*
>
> *Weaknesses:*

> *Although resolving the crystal structure of Ym2 in particular is a strength of the authors work, the weaknesses are that further work or even discussion of Ym2 versus Ym1 has not been directly demonstrated. The authors suggest Ym2 crystals will likely function the same as Ym1, but there is insufficient discussion (or data) beyond sequence similarity as to why this is the case. If Ym1 and Ym2 crystals function the same way, from an evolutionary point, why do mice express two very similar proteins that are expressed under similar conditions that can both crystalise and as the authors suggest act in a similar way. Some discussion around these points would add further value.*

We agree with reviewer. We have further elaborated the discussion section including these points, stating clearly that more research needs to be done using Ym2 crystals before we can draw parallels in vivo.

> *Additionally, the crystal structure for Ym1 has been previously resolved (Tsai et al 2004, PMID 15522777) and it is unclear whether the data from the authors represents an advance in the 3D structure from what is previously known.*

The crystal structure of Ym1 has indeed been previously solved, and we refer to that paper. In addition, we also provide the crystal structure of in vitro grown Ym1, ashowing biosimilarity. This, for the field of crystallography is a major finding, since it validates the concept that crystal structures generated in vitro can reflect in vivo grown structures. Moreover, the in vivo crystallization of Ym2 was unknown prior to this work, and is now clear as revealed by the ex vivo X-ray crystallography. The strength of our story is that we can now compare Ym1 and Ym2 crystals structures in detail.

> *Whilst also generating a model to understand Charcot-Leyden crystals (CLCs), the authors fail to discuss whether crystal shape may be an important feature of crystal function. CLCs are typically needle like, and previous publications have shown using histology and TEM that Ym1 crystals are also needle like. However, the crystals presented in this paper show only formation of plate like structures. It is unclear whether these differences represent different methodologies (ie histology is 2D slides), or differences in CLP crystals that are intracellular versus extracellular. These findings highlight a key question over whether crystal shape could be important for function and has not been addressed by the authors.*

In contrast to the bipyramidal, needle-like CLC crystals formed by human galectin-10 protein (hexagonal space group P6522), the in vivo grown Ym1 and Ym2 crystals we were able to isolate for X-ray diffraction experiments had a plate-like morphology with identical crystallographic parameters as recombinant Ym1/Ym2 crystals (space group P21). We note that depending on the viewing orientation of the thin plate-like Ym1 crystals, they may appear needle-like in histology and TEM images. In addition, we can fully not exclude that both Ym1 or Ym2 may crystallize in vivo in different space groups (which could result in different crystal morphologies for Ym1/Ym2) but we have no data to support this. It is finally also a possibility that plate like structures can break up in vivo along a long axis as a result of mechanical forces, and end up as rod-or needle like shapes.

> *Ym1/Ym2 crystals are often observed in conditions where strong eosinophilic inflammation is present. However, soluble Ym1 delivery in naïve mice shows crystal formation in the absence of a strong immune response. There is no clear discussion as to the conditions in which crystal formation occurs in vivo and how results presented in the paper in terms of priming or exacerbating an immune response align with what is known about situations where Ym1 and Ym2 crystals have been observed.*

Although Ym1 and Ym2 crystals are often observed in mice at sites of eosinophilic inflammation, they are not made by eosinophils, but mainly by macrophages and epithelial cells, respectively. In vitro, protein crystallization typically starts from supersaturated solutions that support crystal nucleation. Several factors such as temperature and pH can affect the solubility of Ym1 and Ym2 in vivo and thus affect the nucleation and crystallization process. For Ym1 and Ym2 we noticed in vitro that a small drop in pH facilitates the crystallization process. Although the physiological pH is 7.4, during inflammation, there is a drop in pH. This drop in pH is the result of the infiltration and activation of inflammatory cells in the tissue, which leads to an increased energy and oxygen demand, accelerated glucose consumption via glycolysis and thus increased lactic acid secretion. In addition, we cannot exclude that in vivo, the nucleation process for Ym1/Ym2 is facilitated by interaction with ligands in the extracellular space (e.g. polysaccharide ligands or other – yet to be identified – specific ligands to Ym1/Ym2).

> ***Reviewer #2 (Public Review):***
>
> *Summary:*
>
> *This interesting study addresses the ability of Ym1 protein crystals to promote pulmonary type 2 inflammation in vivo, in mice.*
>
> *Strengths:*
>
> *The data are extremely high quality, clearly presented, significantly extending previous work from this group on the type 2 immunogenicity of protein crystals.*
>
> *Weaknesses:*
>
> *There are no major weaknesses in this study. It would be interesting to see if Ym2 crystals behave similarly to Ym1 crystals in vivo. Some additional text in the Introduction and Discussion would enrich those sections.*

We agree that this would be interesting to investigate, however, we choose to not include recombinant Ym2 crystal data in this report. However, we have further elaborated the discussion section including this point.

> ***Recommendations for the authors:***
>
> ***Reviewer #1 (Recommendations For The Authors):***
>
> *Suggestions for improved experiments and to strengthen findings:*
>
> *I think additional data on the ability of Ym2 crystals to induce an immune response would be advantageous. I'm not by any means suggesting the authors repeat all the experiments with Ym2 crystals, but even just the ability to show that Ym2 could promote type 2 immunity in the acute OVA model, would help to strengthen the argument that these crystals in general function in a similar way. Alternatively, a discussion on whether these protein crystals may function in different scenarios/tissues or conditions could help in light of additional data*

We agree that this is an interesting point to investigate, however, we choose to not include recombinant Ym2 crystal data in this report. However, we have further elaborated the discussion section including this point.

> *Measuring IL-33 in lung tissue is difficult to interpret as cells will express intracellular IL-33 that is not active and may explain why the results in Fig 2D are not overly convincing.*

> *It could just be that Ym1 crystals are changing the number of cells expressing IL-33 (e.g macrophages, or type 2 pneumocytes) Did the authors also measure active IL-33 release in the BAL fluid which may give a better indication of Ym1's ability to activate DAMPs?*

We also measured active IL-33 release in the BAL fluid, but due to the limited sample availability we could only measure this in one of the two repeat experiments, resulting in non-significant results for the BAL fluid. However, certainly for the 6h timepoint we saw a similar trend in the BAL fluid as in the lung tissue, meaning higher levels of IL-33 in the Ym1 crystal group compared to the PBS and soluble Ym1 group.

> *Crystals in Fig 2F staining with Ym1 appear to be brighter in the soluble Ym1 group. Is this related to increased packing of Ym1 in the crystals formed in vivo as opposed to those formed in vitro? Aside from reduced amount of crystals that form when you give soluble Ym1, could the type of crystal also be influencing the ability of soluble Ym1 crystals to generate an immune response?*

Our X-ray diffraction experiments show that the packing of Ym1 is identical for in vivo and in vitro grown crystals. Possibly the apparent difference in brightness is caused by stochastic staining by the antibody. In this regard we note that the crystals formed from soluble Ym1 after 24h also can appear as less bright in a similar fashion as recombinant Ym1 crystals.

> *Overall, the data and writing of the manuscript is presented to a very high standard*
>
> *A few minor points:*
>
> - *Fig 2F - a little unsure what the number in the left top corner of the images represented.*

These numbers represent the picture numbers generated by the software, but as they don't have any added value for the story, we removed these numbers from the images.

> - *Not clear why two different expression vectors were used - one for Ym1 and one for Ym2?*

Because we observed that recombinant Ym2 is more poorly secreted in the mammalian cell culture supernatant as compared to recombinant Ym1, we produced Ym2 with an N-terminal hexahistidine-tag followed by a Tobacco Etch Virus (TEV)-protease cleavage site to facilitate its purification.

> ***Reviewer #2 (Recommendations For The Authors):***
>
> *The authors briefly outline in their Introduction potential Sources of Ym1/2 in vivo, highlighting monocytes, M2 macrophages, alveolar macrophages, neutrophils and epithelial cells. Do DCs also make detectable/meaningful amounts of Ym1/2 in vivo, particularly in type 2 settings?*

In the introduction we only highlighted the main cellular sources of Ym1 and Ym2, but there is literature available stating/showing that Ym1/2 is not only expressed by macrophages, neutrophils, monocytes and epithelial cells, but can also be induced in DCs and mast cells. We added the word 'mainly' to this sentence in the introduction, to make clear that macrophages, neutrophils and monocytes are not the only sources of Ym1.

> *Given the nicely demonstrated similarity of recombinant Ym1 and Ym2 crystals, I think it is important for the authors to include at least initial data on the outcome of*

> *recombinant Ym2 crystal admin to mice, in comparison to their Ym1 data.*

We agree that this is an interesting point to investigate, however, we choose to not include recombinant Ym2 crystal data in this report. However, we have further elaborated the discussion section including this point.

> *Given the generation of crystals following in vivo administration of soluble Ym1, albeit at a lower level than when crystals were administered, it would be interesting to see if increased concentrations of soluble material show a dose dependent increase in lung inflammation readouts.*

We agree that this would be an interesting point to investigate. Alongside this we could also titrate down the crystal dose, to see if there is a dose dependent decrease in lung inflammation readouts. However, at this time, we choose to not investigate this further.

> *I couldn't easily follow the authors' Discussion about potential ability of anti Ym-1/2 Abs to dissolve Ym1/2 crystals (similar to what they have demonstrated for Abs vs Gal10 crystals). Have they addressed this possibility experimentally? If so, addition of such data to the manuscript would be extremely interesting, given the obvious potential Ym1/2 crystal dissolving Abs for investigation of the role of these in a range of different murine models of type 2 inflammation.*

We agree that the phrasing of this part of the discussion can be unclear/confusing. We rephrased this part to make it clearer. However, we did not address the possibility of Ym1/2 crystal dissolving antibodies experimentally.

> *In the Results section, the authors briefly comment on the pro-type 2 nature of Ym1 crystals in relation to their previous work with uric acid and Gal10 crystals, proposing that the pulmonary type 2 response may be a 'generic response to crystals of different chemical composition'. The Discussion would be enriched by deeper exploration of this comment.*

We have further elaborated the discussion section including this point.